



Near-Collapse Probability of RC Frames in Indonesia Under Repeated Earthquakes Containing Fling-Step Effect

Ade Faisal^{1*}, Afiful Anshari¹, Fadzli Mohamed Nazri², Moustafa Moufid Kassem²

¹*Program Studi Teknik Sipil, Universitas Muhammadiyah Sumatera Utara, Jl. Mukhtar Basri No.3, Medan 20238, Indonesia*

²*School of Civil Engineering, Engineering Campus, Universiti Sains Malaysia, 14300, Nibong Tebal, Penang, Malaysia*

Abstract. The velocity pulse and displacement fling-step pulse signatures may be present in a near-field earthquake ground motion record. It is generally known that near-field ground motion with pulse effects accelerated the building drift. The damage of building can also occur as a result of two or three earthquakes within the building's lifespan. The repeated earthquakes could cause minor to severe damage to the building, including structural collapse. This includes earthquakes with fling-step pulse, which impact is underexamined in the existing studies. Therefore, the objective of this study is to assess the impact of repeated earthquakes with displacement of the fling-step pulse on the near-collapse probability of 5-, 10-, 15 and 20-story concrete frames. Based on the response modification factor $R = 8, 5, \text{ and } 3$, the frames are classified as special, intermediate, and ordinary, respectively. The result shows that the near-collapse probability of repeated earthquakes is more likely to occur on the concrete frames which reaches intensity measure of 27.0% than the effect of single earthquakes.

Keywords: Incremental dynamic analysis; Interstory drift; Nonlinear response history analysis; Probability of near-collapse

1. Introduction

Indonesia is flanked by tectonic plates and is repeatedly experiencing devastating earthquakes due to plate movement. The collision of Eurasian and Indo-Australian plates has produced devastating earthquakes of the West coast of Sumatera, i.e. $M_w > 9.0$ in the Northern part (Prakoso *et al.*, 2017) and $M_w > 8.0$ in the Southern part (Mase, 2018). In the Lombok region of central Indonesia, the collision of these plates has caused earthquakes with $M_w > 7.0$ (Pramono *et al.*, 2018). These types of earthquakes tend to occur repeatedly in the same tectonic region with return periods of hundreds or tens of years, or even shorter. One of the instances is the $M_w 6.4$ earthquakes that is followed by $M_w 6.8$ one which struck the Lombok region on 07/29/18 and 08/05/2018, respectively (Pramono *et al.*, 2018).

A study of reinforced concrete (RC) frames subjected to high vibration found a clear link between interstory drift and structural failure. When the interstory drift reaches 3% in a 10-story RC building, the column sustains initial damage (Dymiotis *et al.*, 1999).

*Corresponding author's email: adefaisal@umsu.ac.id, Tel.: +62-812-6575456; Fax: +62-61-6625474
doi: [10.14716/ijtech.v14i2.4989](https://doi.org/10.14716/ijtech.v14i2.4989)

A severe earthquake causes a significant interstory drift of 2% at level 7 of a 10-story RC building, according to [Kappos and Manafpour \(2001\)](#). These studies, however, are based on a single earthquake's damage state. Recent studies show that the repeated earthquakes on the same site causes more extensive damage to the structures ([Amadio, Fragiacomio, and Rajgelj, 2003](#)). According to [Hatzigeorgiou and Liolios \(2010\)](#) and [Faisal, Majid, and Hatzigeorgiou \(2013\)](#), successive earthquakes cause more damage to multi-story moment resistant frames than a single earthquake ([Di Trapani and Malavisi, 2019](#); [Amiri and Rajabi, 2018](#); [Tahara et al., 2017](#); [Hatzivassiliou and Hatzigeorgiou, 2015](#)).

The fragility curves of 9 RC frames, which are designed according to the seismic code, are investigated by [Kalantari and Roohbakhsh \(2019\)](#). In this study, the near-collapse and collapse limit states due to repeated earthquakes are evaluated as well. [Oggü and Gopikhrisna \(2020\)](#) investigates the probability of collapse of regular and irregular RC structures affected by repeated earthquakes. It shows that the intensity measure for the probability of collapse (IM) of the regular structure is 3.33% less than IM caused by a single earthquake. More recently, [Di Sarno and Pugliese \(2021\)](#) reports that the effect of repeated earthquakes on the existing RC structures increases seismic vulnerability to 17%. Nevertheless, a lower IM result is also found in the study of the probability of collapse due to repeated earthquakes in an existing 4-story RC structure in comparison with the effect of a single earthquake ([Aljawhari et al., 2021](#)).

The earthquake ground motion can be divided into two groups: far field motion (FF) and near-field motion (NF) ([Faisal, Riza, and Hadibroto, 2018](#); [Kalkan and Kunnath, 2006](#)). The near-field ground motion is defined as the earthquake ground motion that is recorded in a seismic station that is less than 15 kilometers away from the ruptured fault zone. It has distinct signatures in both its velocity and displacement forms, (Figure 1), which is unobservable in the far-field motion. Numerous sources already discussed the major impact of near-field ground motion with pulse (or fling-step) on the multi-story RC frames (e.g., [Rashidi et al., 2019](#); [Zahid, Majid, and Faisal, 2017](#); [Champion and Liel, 2012](#); [Majid et al., 2010](#)). However, these studies do not particularly explain the effect of the displacement fling-step pulse on the concrete frames.

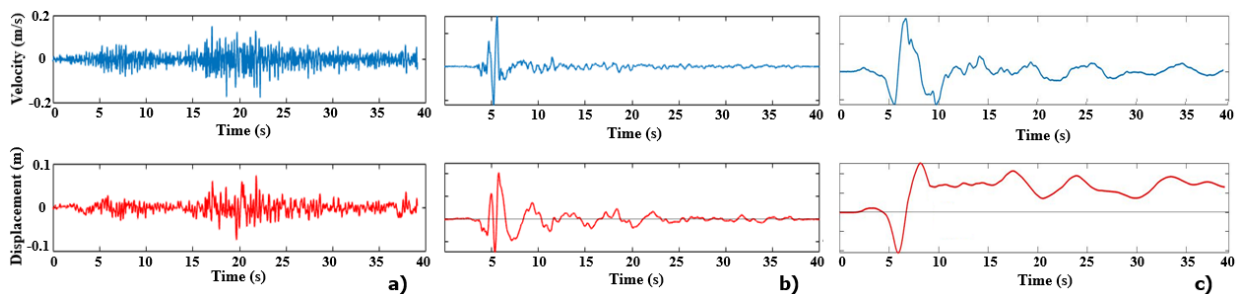


Figure 1 a) far-field earthquake, b) near-field earthquake with velocity pulse effect, and c) near-field earthquake with the displacement fling-step effect

In addition, the influence of a repeated near-field earthquake propagates a bigger drift as compared to the effect of a single earthquake. Again, the effect of multiple earthquakes incorporating only near-field ground motion is not properly investigated yet, especially the impact of multiple earthquakes containing the displacement fling-step pulse on the RC frames. This is, partially, due to the limited available records. Therefore, the aim of this research is to determine the likelihood of near-collapse of the RC frames when subjected to a sequence of near-field earthquakes containing the displacement fling-step effect. The case study is based on the RC frames that are designed and built in Indonesia.

2. Methodology

2.1. RC Frame Model

The evaluated archetype moment resisting frames consists of 5-, 10-, 15- and 20-story RC structures with regular shape of floor plans, masses, and stiffness (Figure 2a and 2b). This study assumes that the RC special moment resisting frame (MRF) with $R = 8$ is constructed on soft soil in Banda Aceh City, Indonesia, whilst the intermediate and ordinary MRFs with $R = 5$ and 3 , respectively, are constructed on medium and hard soils in the same city. The structural model's plan view and the model's frame section are shown in Figure 2. The length of all beams are equivalent at 6.0 m, and the height of all columns is 3.5 m, with the exception of the bottom floor, where the column height is 4.5 m. The concrete and rebar yield strengths used in all models are $f_c' 40$ MPa and $f_y 400$ MPa. The natural period of the structural model is 0.41 s, 0.80 s, 1.16 s, and 1.58 s for 5-, 10-, 15-story, and 20-story RC frames, respectively.

2.2. Elements Strength

The element strength and deformation capacity, which is commonly calculated through the concrete section analysis, is defined based on the FEMA method. Although the internal elastic of the element is designed by flexural force, the yield flexural strength (M_y) of the element is calculated using the empirical value of $1.13M_y$ provided by [Haselton *et al.* \(2010\)](#) to be the maximum flexural force. In order to comply with the code requirement for a strong column weak beam mechanism, the element's flexural forces are adjusted. The Modified-Takeda hysteresis rule is employed to control the material nonlinearity during cycle loads (Figure 2c). The unloading and reloading parameters for beam and column members based on some experimental works on the RC structures are selected, namely $\alpha = 0.3$ and $\beta = 0.6$, respectively, as suggested by [Fardis \(2007\)](#).

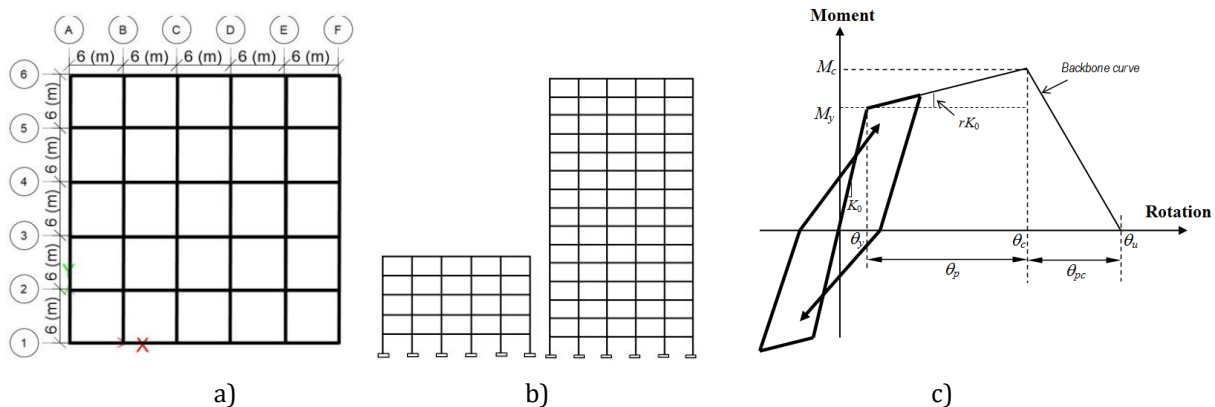


Figure 2 a) The plan view, b) 2D frame models, and c) Modified-Takeda hysteresis and its backbone curve for lumped plasticity model of nonlinear inelastic elements.

2.2. Rotation Capacity

The yield rotation (θ_y) of the member was obtained by the ratio of M_y with elastic rotation stiffness ($K_0=6EI/L$) of the member. The post-yield stiffness ratio or bi-factor (r) of the member's hysteresis rule was estimated based on the ratio of the capping moment and yield moment (M_c/M_y) and ductility of plastic rotation capacity ($\mu_{\theta,c}$), as follows:

$$r = \frac{M_c - M_y}{K_0(\mu_{\theta,c} - 1)\theta_y} \tag{1}$$

Where $\mu_{\theta,c} = \theta_c / \theta_y = (\theta_y + \theta_p) / \theta_y$ and $\theta_y = M_y / K_0$

This study employs plastic rotation capacity $\theta_p = 0.04$ rad for special MRF, whereas $\theta_p = 0.02$ rad for medium and ordinary MRFs, as proposed by Haselton *et al.* (2010). The post capping rotation, θ_{pc} , uses 0.06 based on the average value in Zareian and Krawinkler (2010). The ratio of M_c/M_y reflects the strength hardening of RC members, which is taken as $M_c/M_y=1.13$ based on the average value in Haselton *et al.* (2010), and as suggested by FEMA-P695 (FEMA, 2009).

2.3. Strength Degradation

This study considers the strength degradation of the member up to residual strength of 1% of the initial strength (yield moment) at the ultimate rotation ductility, $\mu_{\theta,u}$. The strength at 1% of the initial strength is sufficiently very low to represent strength at collapse state (Carr, 2010). The capping rotation ductility, $\mu_{\theta,c}$, is defined through Equation 2; whereas ultimate rotation ductility, $\mu_{\theta,u}$, is obtained based on yield rotation (θ_y), plastic rotation capacity (θ_c), and post-capping rotation capacity (θ_{pc}), as follows:

$$\mu_{\theta,u} = \frac{\theta_u}{\theta_y} = \frac{\theta_y + \theta_p + \theta_{pc}}{\theta_y} \quad (2)$$

2.4. Ground Motions and Intensity Measure

Generally, there are 2 types of ground motions employed in earthquake sequence study on the structural response, namely as-recorded mainshock-aftershock and artificial repeated earthquake. Since the as-recorded mainshock-aftershock sequences for motions containing fling-step pulse are scarce, therefore, the ground motion used in this study is artificially repeated earthquakes. These ground motions are selected from the available records in *Pacific Earthquake Engineering Research (PEER) Next Generation Attenuation (NGA)* and *COSMOS*. The selection criteria are based on magnitude, near-field source-to-site distance (≤ 15 km), fault mechanism, and soil type. Table 1 shows the selected records containing near-field motion with fling-step effects.

Table 1 List of selected records of near-field ground motion containing fling-step pulse effect sourced from PEER NGA and COSMOS

Record No	Year	Earthquake	M _w	Station	Dist.(km)	PGA (g)	PGV (cm/s)	PGD (cm)
1	1999	Chi-Chi	7.6	TCU052	1.8	0.35	178.00	493.52
2	1999	Chi-Chi	7.6	TCU068	3.0	0.50	277.56	715.82
3	1999	Chi-Chi	7.6	TCU074	13.8	0.59	68.90	193.22
4	1999	Chi-Chi	7.6	TCU084	11.4	0.98	140.43	204.59
5	1999	Chi-Chi	7.6	TCU129	2.2	0.98	66.92	126.13
6	1999	Kocaeli	7.4	Yarimca	3.3	0.23	88.83	184.84
7	1999	Kocaeli	7.4	Izmit	4.3	0.23	48.87	95.49
8	1999	Chi-Chi	7.6	TCU102	1.2	0.29	84.52	153.88
9	1999	Chi-Chi	7.6	TCU089	8.3	0.34	44.43	193.90
10	1999	Chi-Chi	7.6	TCU049	3.3	0.27	54.79	121.77
11	1999	Chi-Chi	7.6	TCU067	1.1	0.48	94.31	181.25
12	1999	Chi-Chi	7.6	TCU075	3.4	0.32	111.79	164.36
13	1999	Chi-Chi	7.6	TCU076	3.2	0.33	65.93	101.65
14	1999	Chi-Chi	7.6	TCU072	7.9	0.46	83.60	209.67
15	1999	Chi-Chi	7.6	TCU065	2.5	0.76	128.32	228.41
16	1999	Chi-Chi	7.6	TCU078	8.3	0.43	41.88	121.23
17	1999	Chi-Chi	7.6	TCU082	4.5	0.22	50.49	142.78
18	1999	Chi-Chi	7.6	TCU128	9.1	0.14	59.42	91.05
19	1999	Chi-Chi	7.6	TCU071	4.9	0.63	79.11	244.05
20	1994	Northridge-01	6.7	LA-Sepulveda	6.7	0.46	13.80	26.13

The intensity measure (IM) employed in this study is $RSA(T_1)$. All the selected records are scaled up and down by referring to the elastic designed spectral acceleration (Figure 3a) at the natural period of the model considered, $RSA(T_1)$, as demonstrated in Figure 3b. The design spectra for Banda Aceh City is depicted in Figure 3a, which is developed based on the Indonesian seismic code (SNI 1726:2012) (BSN, 2012). The Indonesian code is originally adopted from standard ASCE/SEI 7-10 (ASCE, 2013). In order to model the artificial repeated earthquakes, all the scaled ground motions are then paired randomly by adding the 50 seconds of zero motions in between two, and/or three scaled motions (Figure 3c) to make the free vibration on the structure exhibit properly before the next earthquake motion started. The study used single, 2- and 3-times repeated earthquakes to be induced on the RC moment resisting frames (MRF) model.

2.5. Structural Analysis and Collapse Limit State

In the design phase, the two dimensional of 3-, 10-, 15 and 20-story RC frames are analyzed with the response spectrum method to get the design flexural force. The elastic design phase complies with the Indonesian Standard SNI 1726:2012 (BSN, 2012), which is nearly identical with the ASCE/SEI 7-10 (ASCE, 2013). The 2D nonlinear inelastic response history analysis with lumped plasticity model is conducted to define the near-collapse state of the system using Ruaumoko 2D v.4.0 (Carr, 2010). This analysis is done in line with the seismic performance assessment guideline as stipulated in FEMA P-695 (FEMA, 2009).

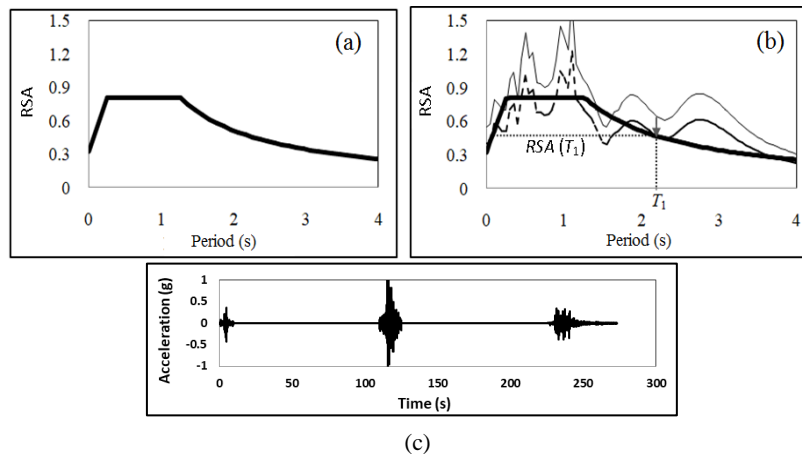


Figure 3 Model of earthquake ground motion: a) Elastic design spectra for Banda Aceh City, b) Illustration of the ground motion scaling process, (c) example of 3 times repeated earthquakes

The incremental dynamic analysis (IDA) (Vamvatsikos & Cornell, 2002) is utilized to define the interstory drift (IDR) for the near collapse state, which is the same as the engineering demand parameter (EDP). In the IDA, the $IM = RSA(T_1)$ is repeatedly scaled in order to find the IM level at which each ground motion causes EDP's failure criterion such as near-collapse or collapse. The near-collapse limit state of $IDR = 2.0\%$ is employed based on the requirement stipulated in Indonesian seismic code, as well as in ASCE 7-10. From IDA, the following parameters namely, μ and β , median and standard deviation, respectively, are defined by fitting the interpolated IM through the method of moments as follow:

$$\log[\mu_{RSA(T_1)}] = \frac{1}{n} \sum_{i=1}^n \log[RSA(T_1)]_i \quad (3)$$

$$\beta_{\log[RSA(T_1)]} = \sqrt{\frac{\sum_{i=1}^N (\log[RSA(T_1)] - \log[\mu_{RSA(T_1)}])^2}{N-1}} \quad (4)$$

2.6. Probability of Near Collapse

The probability of near collapse (or any limit state of interest) is commonly expressed by the fragility function, which is developed through a log normal cumulative distribution function as follows:

$$P[D \geq d | R = RSA(T_1)] = \Phi \left(\frac{\log(RSA(T_1) / \mu_{RSA(T_1)})}{\sqrt{\beta_{\log[RSA(T_1)]}^2 + \beta_u^2}} \right) \quad (5)$$

where $P[D \geq d | R = RSA(T_1)]$ is the probability of reaching or exceeding the collapse state (the so-called probability near collapse), while the structure is induced by a ground motion with $R = RSA(T_1)$; $\Phi(\cdot)$ is the standard lognormal cumulative distribution function; $\mu_{RSA(T_1)}$ is the median of the ground motion that will cause collapse; and $\beta_{\log[RSA(T_1)]}$ is the standard deviation of the ground motion that will cause near-collapse. In developing the fragility function, the result from the IDA doesn't always achieve the targeted collapse limit state. A statistical tool proposed by Baker (2015) is useful to repair the data in order to estimate the fragility function. The study also adopts the recommendation of FEMA P-58 guidelines in order to always increase the logarithmic standard deviation (by adding $\beta_u = 0.1$). It is done so since the uncertainty in the analytically-based fragility curve could not adequately and accurately represent the true variability (Porter, Kennedy, and Bachman, 2007).

3. Results and Discussion

This section is discussed based on the median value of probability near collapse, $\mu_{RSA(T_1)}$, to capture the increment of effect of the repeated earthquake on the system. Moreover, the standard deviation of the cumulative distribution of $IM = RSA(T_1)$, $\beta_{IM} = \sqrt{\beta_{\log[RSA(T_1)]}^2 + \beta_u^2}$, is also used to discuss the decrease of IM required to produce near-collapse state. This value will affect the slope of the diagonal line of fragility curve. The result of $\mu_{RSA(T_1)}$ and β_{IM} that are used to construct the fragility curve is provided in Table 2. The table indicates that β_{IM} is found within the range of 0.16 to 0.33 for all MRFs considered in the study. Porter, Kennedy, and Bachman (2007) find that commonly β_{IM} is within the range of 0.2 to 0.6, after adding the uncertainty factor β_u , whereas Baker (2015) explains that $\beta = 0.4$ is commonly used to develop the fragility function, without the uncertainty factor. Basone et al. (2017) assess the seismic fragility curve of RC buildings with $T_1 = 0.34$ s and find the standard deviation for the dataset, which ranged from 0.29 to 0.60. They evaluate the RC building up to the collapse state. Porter et al. also explains that the quality of the dataset is high if the μ or β differences are found to be $\geq 20\%$. The μ and β listed in Table 2 clearly demonstrates the value difference, as indicated by Porter et al. Therefore, it can be said that the $\mu_{RSA(T_1)}$ and β_{IM} resulted from this study is well defined, thus it is capable to produce high quality fragility functions.

Figures 4 - 6 have depicted the fragility curve of the 5-, 10-, 15-, and 20-story of special (R=8), intermediate (R=5), and ordinary (R=3) MRFs under the effect of single earthquake (1XE), 2-times earthquake (2XE) and 3-times earthquakes (3XE). Overall, the figures clearly demonstrate that as the number of stories and R increased, the IM required to produce near-collapse state decreased. This rule of thumb confirms that the process conducted in

this study is in the right path. Figure 4a indicates that $IM = RSA(T_1) = 2.63$ g is required to achieve the probability of near-collapse for 5-story ordinary MRF. This IM is slightly decreased to 2.38 g and 2.30 g for 2XE and 3XE, respectively, to achieve near-collapse probability. A similar condition is also indicated in 10- and 20-story ordinary MRFs in achieving the probability near-collapse (Figures 4b and 4c). For this ordinary MRF, the maximum effect of 2XE and 3XE is found to be exhibited on the 15-story and 20-story MRFs, respectively. In average, the 2XE has influenced the response of 15-story MRF to be 14.48% more likely than 1XE in achieving the near-collapse state, whereas 3XE has affected 20-story MRF of 24.4% more likely than 1XE (Figures 4c and 4d).

Table 2 Statistical parameters for the fragility function of near-collapse state

Earthquake	MRF Story (Fund. Period)	R=8		R=5		R=3	
		$\mu_{RSA(T_1)}$	σ_{IM}	$\mu_{RSA(T_1)}$	σ_{IM}	$\mu_{RSA(T_1)}$	σ_{IM}
1x Earthquake	5 ($T_1=0.41$ s)	1.56	0.29	2.10	0.21	2.62	0.17
	10 ($T_1=0.80$ s)	0.85	0.35	1.00	0.33	1.22	0.30
	15 ($T_1=1.16$ s)	0.58	0.32	0.70	0.27	0.70	0.26
	20 ($T_1=1.58$ s)	0.36	0.33	0.43	0.30	0.45	0.32
2x Earthquake	5 ($T_1=0.41$ s)	1.33	0.27	1.90	0.22	2.38	0.16
	10 ($T_1=0.80$ s)	0.66	0.33	0.82	0.28	0.95	0.29
	15 ($T_1=1.16$ s)	0.51	0.29	0.57	0.24	0.52	0.37
	20 ($T_1=1.58$ s)	0.30	0.28	0.32	0.28	0.45	0.32
3x Earthquake	5 ($T_1=0.41$ s)	1.16	0.23	1.80	0.21	2.30	0.16
	10 ($T_1=0.80$ s)	0.57	0.28	0.77	0.28	0.92	0.27
	15 ($T_1=1.16$ s)	0.51	0.29	0.50	0.23	0.60	0.21
	20 ($T_1=1.58$ s)	0.25	0.27	0.30	0.23	0.36	0.31

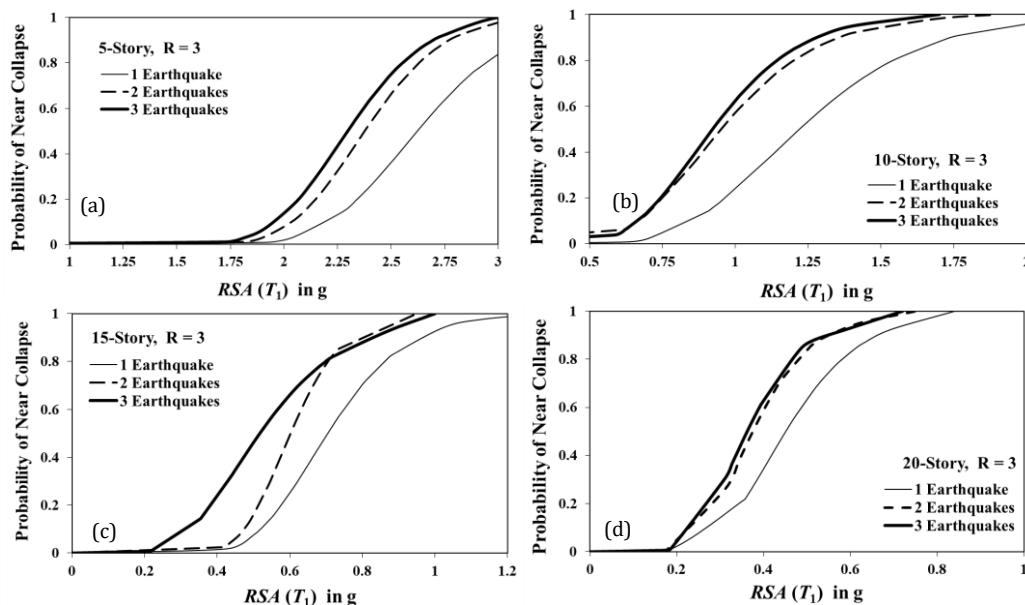


Figure 4 Probability of near collapse for 5-, 10-, 15-, and 20-story RC frames for R = 3 induced by repeated earthquake with fling-step effects

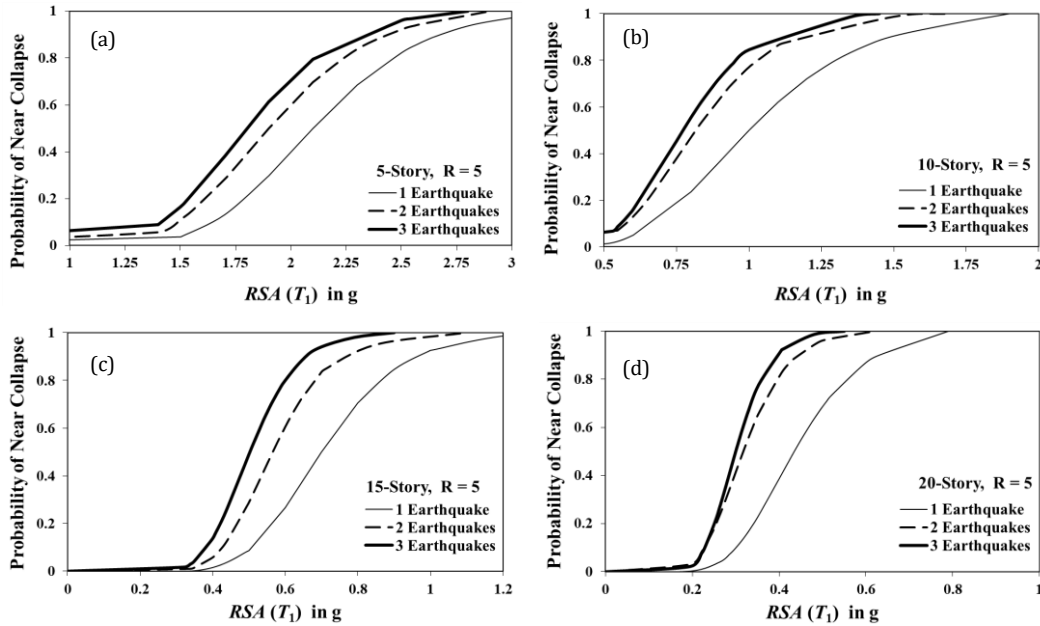


Figure 5 Probability of near collapse for 5-, 10-, 15-, and 20-story RC frames for $R = 5$ induced by repeated earthquake with fling-step effects

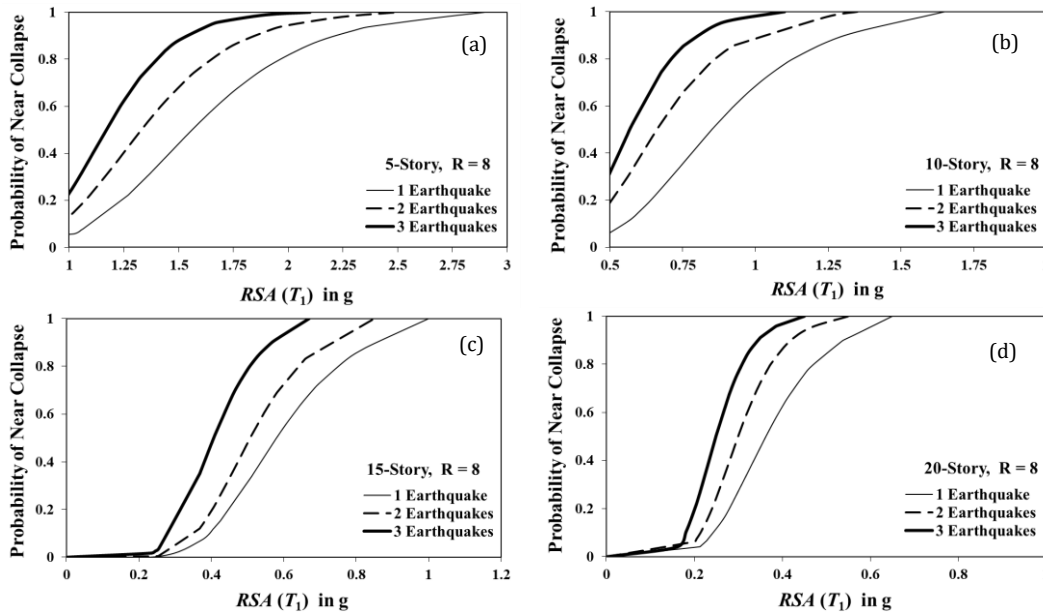


Figure 6 Probability of near collapse for 5-, 10-, 15-, and 20-story RC frames for $R = 8$ induced by repeated earthquake with fling-step effects

The near-collapse probability for intermediate and special MRFs is depicted in Figures 5 and 6, respectively. The figures indicate that the effect of R pushes the diagonal line of the fragility curve to the left to become a vertical-like line. These conditions mean that lower IM is more likely achieve the near-collapse EDP. In the case of intermediate MRF, the study finds that 2XE produces the maximum effect on the 20-story MRF (Figure 5d). The 2XE makes the decrement of IM reached 27.0% in achieving near-collapse EDP, whereas 3XE has maximum affection on the 15-story MRF, which is about 11.13 % more likely than the IM of 1XE (Figure 5c). Similar trend is indicated for special MRFs affected by single and repeated earthquakes in Figure 6. The IM of probability near collapse is clearly decreased as the number of the story increased.

In Table 2, the median for special and intermediate MRFs, which have fundamental periods of $T_1 = 0.41$ s to 1.58 s, are found within the range of $\mu = 0.36$ to 2.10. This result is much lower than the median IDA result of $\mu = 0.98$ to 5.36 for the collapse capacity of modern ductile concrete MRF with $T_1 = 0.42$ s to 1.69 s done by [Champion and Liel \(2012\)](#). It is obviously lower since this study is based on the near-collapse state, which is not the collapse state as reported in Champion and Liel's study. In fact, this study also found the collapse state median IDA of $\mu = 0.71$ to 4.67, which would be discussed in the upcoming paper.

[Kalantari and Roohbakhsh \(2019\)](#) found the fragility curve of the 4-story RC structure is based on the dispersion of $b = 0.82$ to 1.04. Their study also explains that the fragility curve of a 15-story RC structure is developed based on $b = 0.96$ to 1.07. [Aljawhari *et al.* \(2021\)](#) reports that the dispersion of $b = 0.359$ is used to generate the fragility curve of a 4-story RC building. In this study, we obtained $b = 0.27$ for 5-story, and $b = 0.29$ for 15-story RC special MRF. The significant gap shown in result b is mainly caused by the handling of the uncertainty issues (quality of the dataset) for each study. Therefore, the comparison of those results shall not be made straightforward. However, statistically, we may refer to [Porter, Kennedy, and Bachman \(2007\)](#) and [Baker \(2015\)](#) for the common thresholds of dispersion in developing fragility curves, i.e. $b = 0.2$ to 0.4. It means that the fragility curves of this study and the one in the study of Aljawhari *et al.* are the common curves to be used as the probability of the limit state function of RC structures.

[Shokrabadi, Burton, and Stewart \(2018\)](#) already explains that the response RC frames with $T_1 = 1.12$ s and 1.71 s are increased significantly to 30% - 50% when aftershock combines with mainshock motions. This increases the collapse probability to be 1.5 and 3.5 times more likely. The evaluation of a 4-story regular RC frame made by [Oggü and Gopikhrisna \(2020\)](#) finds that the probability of the considered IM decreases to 23.91%, which is smaller than the effect of a single earthquake. [Di Sarno and Pugliese \(2021\)](#) reported that the effect of repeated earthquakes on existing 4-story RC structures caused the probability of considered IM to decrease to 17% in comparison with the effect of a single earthquake. In this study, the probability of IM for 5-story RC special MRF under repeated earthquakes is decreased to 25.94%, which is smaller than the effect of a single earthquake. These significant gaps in the probability of IMs are mainly caused by the different methods of modeling the repeated earthquake and the selection of ground motion.

4. Conclusions

The probabilistic seismic assessment of reinforced concrete (RC) moment resisting frame (MRF) in Indonesia has been presented. The assessment makes use of the single, twice, and three times repeated earthquakes (referred to as 1XE, 2XE, and 3XE) that contain the displacement fling-step pulse. Four archetype RC frames were considered, namely 5-, 10-, 15-, and 20-story with response modification factor $R = 8, 5,$ and 3, which represents special, intermediate, and ordinary MRF. Therefore, this study concluded that repeated earthquakes is more likely producing near-collapse IM 27.0% earlier than the IM of single earthquake, particularly on the intermediate MRF. In this case, the near-collapse probability of ordinary MRF is posed slightly differently with intermediate MRF. For special MRF, it is found that the near-collapse probability may increase significantly due to the effect of 2XE and 3XE. It is indicated by the 22.19% decrement of IM in producing near-collapse EDP, which was lower than IM for 1XE. In average, the 2XE which might be producing the near-collapse IM of 16.58% is more likely to occur on the all considered RC frames in comparison with 1XE. This probability was larger than 3XE effect, which 9.45% more likely to exhibit on the frames compared with the effect of 1XE. In average, the

repeated earthquakes containing fling-step pulse may increase the near-collapse probability of special, intermediate, and ordinary RC frames to reach 13.81%, 12.67%, and 12.56%, respectively. In comparison to 1XE, the trends of the effect of 3XE on this near-collapse probability do not always produce a superior effect when compared to the effect of 2XE. Indeed, besides the repeated earthquakes containing fling-step pulse, the variations in considered story heights, R , and rotation capacity also contributes to the critical effect on the seismic performance of the structure.

Acknowledgments

We gratefully thank the Fundamental Research grant with contract number 05/II.3-AU/UMSU-LP2M/C/2021 in the year 2021 for sponsoring this study, which were awarded to the first author. The authors wish to thank the undergraduate students who were involved in this research as numerators.

References

- Amadio, C., Fragiaco, M., Rajgelj, S., 2003. The effects of repeated earthquake ground motions on the nonlinear response of SDOF systems. *Earthquake Engineering & Structural Dynamics*, Volume 32(2), pp. 291–308
- Aljawhari, K., Gentile, R., Freddi, F., Galasso, C. 2021. Effects of ground-motion sequences on fragility and vulnerability of case-study reinforced concrete frames. *Bulletin of Earthquake Engineering*, Volume 19(15), pp. 6329–6359
- Amiri, G.G., Rajabi, E., 2018. Effects of consecutive earthquakes on increased damage and response of reinforced concrete structures. *Computers & Concrete*, Volume 21(1), pp. 55–66
- ASCE, 2013. *Minimum Design Loads for Buildings and Other Structures*, ASCE Standard ASCE/SEI 7-10, American Society of Civil Engineers, Reston
- Baker, J.W., 2015. Efficient analytical fragility function fitting using dynamic structural analysis. *Earthquake Spectra*, Volume 31(1), pp. 579–599
- Basone, F., Cavaleri, L., Di Trapani, F., Muscolino, G., 2017. Incremental dynamic based fragility assessment of reinforced concrete structures: stationary vs. non-stationary artificial ground motions. *Soil Dynamics & Earthquake Engineering*, Volume 103, pp. 105–117
- Carr, A.J., 2010. *Ruaumoko Manual Volume: 1, Theory and User Guide to Associated Program*. University of Canterbury
- Champion, C., Liel, A., 2012. the effect of near-fault directivity on building seismic collapse risk. *Earthquake Engineering & Structural Dynamics*, Volume 41(10), pp. 1391–1409
- Di Sarno, L., Pugliese, F. 2021. Effects of mainshock-aftershock sequences on fragility analysis of RC buildings with ageing. *Engineering Structures*, Volume 232, p. 111837
- Di Trapani, F., Malavisi, M., 2019. Seismic fragility assessment of infilled frames subject to mainshock/aftershock sequences using a double incremental dynamic analysis approach. *Bulletin of Earthquake Engineering*, Volume 17(1), pp. 211–235
- Dymiotis, C., Kappos, A.J., Chryssanthopoulos, M.K., 1999. Seismic reliability of RC frames with uncertain drift and member capacity. *Journal of Structural Engineering*, Volume 125(9), pp. 1038–1047
- Faisal, A., Majid, T. A., Hatzigeorgiou, G. D. 2013. Investigation of Story Ductility Demands of Inelastic Concrete Frames Subjected to Repeated Earthquakes. *Soil Dynamics & Earthquake Engineering*, Volume 44, pp. 42–53

- Faisal, A., Riza, F.V., Hadibroto, B. 2018. Global ductility demands of RC frames with various post-yield stiffness ratio and ductility capacity ratio under near-field earthquakes
- Fardis, M.N., 2007. *Guidelines for displacement-based design of buildings and bridge*. Pavia, Italy: IUSS Press
- FEMA, 2009. *Quantification of Building Seismic Performance Factors*. Rep. FEMA P-695, Federal Emergency Management Agency, Washington, D.C
- Hatzigeorgiou, G.D., Liolios, A.A., 2010. Nonlinear behaviour of RC frames under repeated strong ground motions. *Soil dynamics & Earthquake Engineering*, Volume 30(10), pp. 1010–1025
- Hatzivassiliou, M., Hatzigeorgiou, G.D., 2015. Seismic sequence effects on three-dimensional reinforced concrete buildings. *Soil Dynamics & Earthquake Engineering*, Volume 72, pp. 77–88
- Haselton, C.B., Liel, A.B., Deierlein, G.G., Dean, B.S., Chou, J.H., 2010. Seismic collapse safety of reinforced concrete buildings. I: Assessment of ductile moment frames. *Journal of Structural Engineering*, Volume 137(4), pp. 481–491
- Kalkan, E., Kunnath, S.K., 2006. Effects of fling step and forward directivity on seismic response of buildings. *Earthquake Spectra*, Volume 22(2), pp. 367–390
- Kalantari, A., Roohbakhsh, H. 2020. Expected seismic fragility of code-conforming RC moment resisting frames under twin seismic events. *Journal of Building Engineering*, Volume 28, p. 101098
- Kappos, A., Manafpour, A., 2001. Seismic design of R/C buildings with the aid of advanced analytical techniques. *Engineering Structures*, Volume 23, pp. 319–332
- Majid, T.A., Wan, H.W., Zaini, S.S., Faisal, A., Wong, Z.M., 2010. The effect of ground motion on non-linear performance of asymmetrical reinforced concrete frames. *Disaster Advances*, Volume 3(4), pp. 35–39
- Mase, L.Z., 2018, Reliability study of spectral acceleration designs against earthquakes in Bengkulu City, Indonesia, 2018. *International Journal of Technology*, Volume 9(5), pp. 910–924
- National Standardization Agency of Indonesia (BSN), 2012. *Design Code of Earthquake Resistance Structures for Building and Non-Building, SNI 1726:2012*. Jakarta
- Oggu, P., Gopikrishna, K. 2020. Assessment of three-dimensional RC moment-resisting frames under repeated earthquakes. *Structures*, Volume 26, pp. 6–23
- Porter, K., Kennedy, R., Bachman, R., 2007. Creating fragility functions for performance based earthquake engineering. *Earthquake Spectra*, Volume 23, pp. 471–89
- Prakoso, W.A., Rahayu, A., Sadisun, I.A., Muntohar, A.S., Muzli, M., Rudyanto, A., 2017. Comparing shear-wave velocity determined by MASW with borehole measurement at Merapi Sediment in Yogyakarta. *International Journal of Technology*, Volume 8(6), pp. 993–1000
- Pramono, S., Prakoso, W.A., Rohadi, S., Karnawati, D., Permana, D., Prayitno, B.S., Rudyanto, A., Sadly, M., Sakti, A.P., Octantyo, A.P., 2020. Investigation of Ground Motion and Local Site Characteristics of the 2018 Lombok Earthquake Sequence. *International Journal of Technology*, Volume 11(4), pp. 743–753
- Rashidi, A., Majid, T.A., Fadzli, M.N., Faisal, A., Noor, S.M., 2017. A Comprehensive Study on the Influence of Strength and Stiffness Eccentricities to the on-Plan Rotation of Asymmetric Structure. *In: Proceedings of the International Conference of Global Network for Innovative Technology and Awam International Conference in Civil Engineering (IGNITE-AICCE'17): Sustainable Technology and Practice for Infrastructure and Community Resilience*

- Shokrabadi, M., Burton, H.V., Stewart, J. P. 2018. Impact of sequential ground motion pairing on Mainshock-Aftershock structural response and collapse performance assessment. *Journal of Structural Engineering*, Volume 144(10), p. 04018177
- Tahara, R.M.K., Majid, T.A., Zaini, S.S., Faisal, A., 2017. Effect of repeated earthquake on inelastic moment resisting concrete frame. *In: Proceedings of the International Conference of Global Network for Innovative Technology and AWAM International Conference in Civil Engineering*, Penang, 8-9 August, Malaysia
- Vamvatsikos, D., Cornell, C.A., 2002. Incremental dynamic analysis. *Earthquake Engineering & Structural Dynamics*, Volume 31(3), pp. 491-514
- Zahid, M. Z. A. M., Majid, T. A., Faisal, A., 2017. The effect of behaviour factor on the seismic performance of low-rise and high-rise RC buildings. *Journal of Engineering Science and Technology*, Volume 12(1), pp. 031-041
- Zareian, F., Krawinkler, H. 2010. Structural system parameter selection based on collapse potential of buildings in earthquakes. *Journal of Structural Engineering*, Volume 136(8), pp. 933-943